

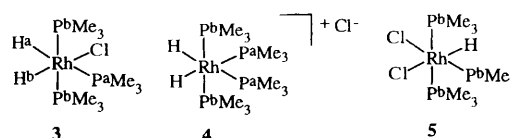
## Dalton Communications

Rapid Characterisation of Rhodium Dihydrides by Nuclear Magnetic Resonance Spectroscopy using Indirect Two-dimensional Methods and *para*-Hydrogen†Simon B. Duckett,<sup>\*a</sup> Graham K. Barlow,<sup>a</sup> Martin G. Partridge<sup>a</sup> and Barbara A. Messerle<sup>b</sup><sup>a</sup> Department of Chemistry, University of York, Heslington, York YO1 5DD, UK<sup>b</sup> Department of Organic Chemistry, University of Sydney, Sydney, NSW 2006, Australia

When  $[\text{RhH}_2(\text{PMe}_3)_3\text{Cl}]$ , incorporating chemically inequivalent hydrides, and  $[\text{RhH}_2(\text{PMe}_3)_4]\text{Cl}$ , containing magnetically inequivalent hydrides, were generated using *para*-enriched hydrogen, their  $^1\text{H}$ - $^{103}\text{Rh}$  and  $^1\text{H}$ - $^{31}\text{P}$  two-dimensional NMR spectra were quickly obtained from < 1 mg of complex with and without the aid of pulsed field gradients.

Enhanced absorption and emission signals have been observed in NMR spectra of nuclei which arise from those of *para*-hydrogen ( $p\text{-H}_2$ ), or possess a direct scalar coupling to these nuclei.<sup>1</sup> The enhancement, termed *para*-hydrogen-induced polarisation (PHIP) by Eisenberg,<sup>2</sup> is a direct result of the destruction of the antisymmetric  $p\text{-H}_2$  spin state, a nuclear singlet, in a spin-correlated chemical process. Such processes occur in catalytic hydrogenation reactions, resulting in large enhancements of NMR signal intensity for hydrogenation products and metal dihydrides.<sup>3</sup> Here we show for the first time that indirect measurements, in conjunction with the use of  $p\text{-H}_2$ , allow the measurement of  $^{31}\text{P}$  and  $^{103}\text{Rh}$  NMR spectra for species present in concentrations of  $\ll 1$  mmol  $\text{dm}^{-3}$ . In addition, we demonstrate that chemically equivalent, but magnetically inequivalent, hydride nuclei in metal dihydrides can be detected by their PHIP signature.

The reaction chemistry concerns the addition of  $\text{H}_2$  to  $[\text{Rh}(\text{PMe}_3)_3\text{Cl}]^4$  **1** and  $[\text{Rh}(\text{PMe}_3)_4]\text{Cl}^5$  **2**. A 1 mg sample of  $[\text{Rh}(\text{PMe}_3)_3\text{Cl}]$  in  $\text{CD}_2\text{Cl}_2$  under 3 atm  $p\text{-H}_2$  was examined at 312 K using a modified heteronuclear multiple quantum correlation (HMQC) experiment.<sup>6</sup> The maximum initial transverse magnetisation obtainable from the two-spin order  $I_{z1}I_{z2}$  product state formed in the  $p\text{-H}_2$  derived product  $[\text{RhH}_2(\text{PMe}_3)_3\text{Cl}]$  **3** arises when the first  $\frac{\pi}{2}(^1\text{H})$  pulse in the HMQC sequence is replaced by a  $\frac{\pi}{4}$  pulse.<sup>1,7</sup> The rest of the sequence,  $-\tau-\frac{\pi}{2}(\text{X})-t_1-\pi(^1\text{H})-t_1-\frac{\pi}{2}(\text{X})-\tau-\frac{\pi}{2}(\text{X})$ -detect ( $^1\text{H}$ ) is identical to that in a standard HMQC experiment in which the magnetisation created by the initial pulse evolves during the fixed delay,  $\tau$ , with respect to heteronuclear couplings, thereby enabling the generation of heteronuclear multiple quantum coherence. The duration of  $t_1$ , the evolution period, is incremented for each slice to build up the two-dimensional data matrix. Phase-sensitive acquisition was achieved using time proportional phase incrementation<sup>8</sup> by incrementing the phase of the first pulse to the heteronucleus (X) by  $\frac{\pi}{2}$  for each slice of the two-dimensional data set. The sequence is completed with a purge pulse. Using this indirect approach we are able to detect the  $^{31}\text{P}$  and  $^{103}\text{Rh}$  nuclei of the  $\text{H}_2$  addition products *via* their most sensitive  $^1\text{H}$  signature (Fig. 1). The hydride resonances at  $\delta -9.79$  and  $-19.5$  are assigned to the ligands,  $\text{H}_a$  and  $\text{H}_b$  of complex **3**.<sup>†</sup> In the  $^1\text{H}$ - $^{31}\text{P}$  correlation spectrum four cross-



peaks are observed connecting each phosphorus centre,  $\text{P}_a$  and  $\text{P}_b$ , to its proton coupling partners, the hydrides  $\text{H}_a$  and  $\text{H}_b$ . The relative intensities of the four cross-peaks depend on the value of  $\tau$ ; when  $\tau = \frac{1}{2}J(\text{P}_a\text{H}_a)$  the strongest cross-peak connects the hydride at  $\delta(^1\text{H}) -9.79$  ( $\text{H}_a$ ) to the phosphorus centre at  $\delta(^{31}\text{P}) -21.3$  [ $\text{P}_a$ , dt,  $J(\text{RhP}_a) = 88$ ,  $J(\text{PP}) = 28$  Hz] and confirms their *trans* arrangement [Fig. 1(a) and 1(c)].<sup>§</sup> The short data-storage time of 25 ms used in this HMQC

† Selected NMR data (in  $\text{CD}_2\text{Cl}_2$ , 500.13 MHz  $^1\text{H}$ , 202.45 MHz  $^{31}\text{P}$  and 15.77 MHz  $^{103}\text{Rh}$ ;  $^{103}\text{Rh}$  spectra, recorded on 5 mm samples in a 10 mm inverse-geometry probe, were referenced relative to 3.16 MHz,  $\delta$  0): **3**,  $^1\text{H}$  (312 K)  $\delta -9.79$  [ $\text{H}_a$ ,  $J(\text{P}_a\text{H}) = 176$ ,  $J(\text{P}_b\text{H}) = -19$ ,  $J(\text{RhH}) = 15$ ,  $J(\text{HH}) = -8$ ] and  $-19.5$  [ $\text{H}_b$ ,  $J(\text{RhH}) = 27$ ,  $J(\text{P}_a\text{H}) = 13$ ,  $J(\text{P}_b\text{H}) = 20$ ,  $J(\text{HH}) = -8$ ];  $^{31}\text{P}$  (312 K)  $\delta -7.4$  [ $\text{P}_b$ , dd,  $J(\text{RhP}_b) = 103$ ,  $J(\text{PP}) = 28$ ] and  $-21.3$  [ $\text{P}_a$ , dt,  $J(\text{RhP}_a) = 88$ ,  $J(\text{PP}) = 28$ ];  $^{103}\text{Rh}$  (312 K)  $\delta -319$  [dt,  $J(\text{RhP}) = 88$ , 103]; **4**,  $^1\text{H}$  (300 K)  $\delta -10.72$  [2 H, m,  $J(\text{PH}_{trans}) = 149$ ,  $J(\text{PH}_{cis}) = 32.7$ ,  $J(\text{RhH}) = 14.5$ ,  $J(\text{P}_b\text{H}) = 20.3$ ];  $^{31}\text{P}$  (300 K)  $\delta -12.6$  [ $\text{P}_b$ , dt,  $J(\text{RhP}_b) = 96$ ,  $J(\text{P}_b\text{P}_a) = 28$ ] and  $-23.6$  [ $\text{P}_a$ , dt,  $J(\text{RhP}_a) = 86$ ,  $J(\text{P}_b\text{P}_a) = 28$ ];  $^{103}\text{Rh}$  (300 K)  $\delta -1007$  [tt,  $J(\text{RhP}_a) = 86$ ,  $J(\text{RhP}_b) = 96$ ]; **5**,  $^1\text{H}$  (300 K,  $\text{CD}_2\text{Cl}_2$ )  $\delta -17.74$  [H,  $J(\text{P}_b\text{H}) = 15$ ,  $J(\text{P}_a\text{H}) = 18.6$ ,  $J(\text{RhH}) = 21.7$ ];  $^{31}\text{P}$  (300 K)  $\delta 8.71$  [ $\text{P}_a$ , dt,  $J(\text{PP}) = 32$ ,  $J(\text{RhP}) = 131$ ] and  $-6.90$  [ $\text{P}_b$ , dd,  $J(\text{RhP}) = 93$ ,  $J(\text{PP}) = 32$  Hz];  $^{103}\text{Rh}$  (300 K)  $\delta 892$ .

§ In all cases one-dimensional  $^1\text{H}$  NMR spectra were first recorded in order to measure the value of  $J(\text{XH})$  used for multiplet selection in the two-dimensional sequence and to optimise the temperature for a given experiment time. For example, at 343 K in  $\text{C}_6\text{D}_6$  the hydrides of complex **3** briefly showed 200-fold enhancement. However, at 312 K, in  $\text{CD}_2\text{Cl}_2$  the initial hydride signal enhancement fell to 30 fold but remained appreciable for up to 20 min. In addition, we independently optimised the recycle time to yield the maximum refreshed signal for each sample/temperature (typically this lies between 20 and 100 ms) and between 1024 and 256 increments were recorded. Only increments stored before the  $p\text{-H}_2$  enhancement drops to zero (no signal) were used in the transformed data. In the two-dimensional spectra passive phosphorus- and rhodium-phosphorus couplings were observed in the second dimension.

† Non-SI unit employed: atm  $\approx 101\,325$  Pa.

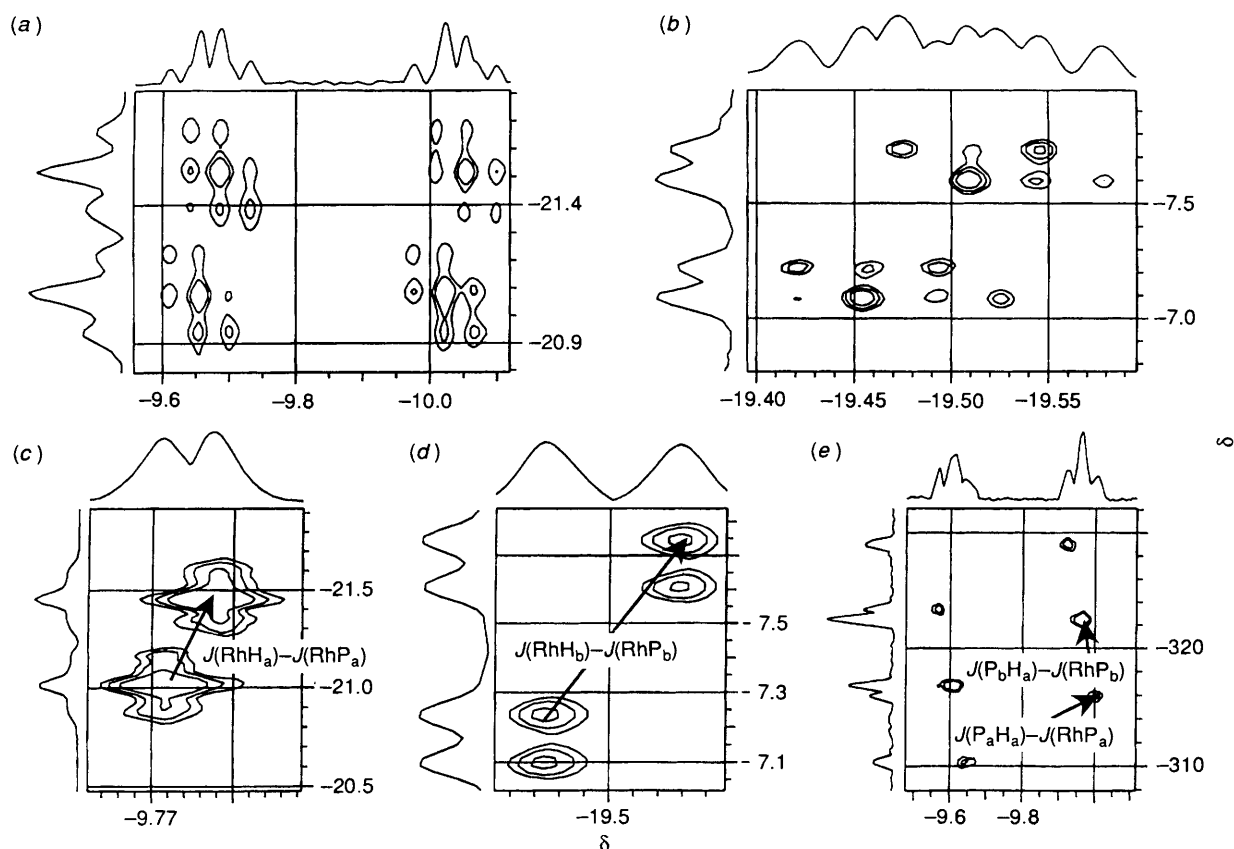


**Fig. 1** Selected cross-peaks (positive contours) and projections from  $^1\text{H}$ - $^{31}\text{P}$  and  $^1\text{H}$ - $^{103}\text{Rh}$  correlation spectra of  $[\text{RhH}_2(\text{PMe}_3)_3\text{Cl}]$  **3**, obtained with  $p\text{-H}_2$  in  $\text{CD}_2\text{Cl}_2$  at 312 K. The slopes of the solid lines reveal the sign of the product of the indicated couplings. (a) The  $^1\text{H}$ - $^{31}\text{P}$  correlation spectrum acquired using  $\tau = \frac{1}{2}J(\text{P}_a\text{H}_a)$ , showing the cross-peak connecting  $\text{H}_a$  to  $\text{P}_a$ ; (b) the  $^1\text{H}$ - $^{31}\text{P}$  correlation spectrum acquired using  $\tau = \frac{1}{2}J(\text{P}_b\text{H}_b)$ , showing the cross-peak connecting  $\text{H}_b$  and  $\text{P}_b$ ; (c) the  $^1\text{H}$ - $^{31}\text{P}$  correlation spectrum,  $^{31}\text{P}$  decoupled, acquired using  $\tau = \frac{1}{2}J(\text{P}_a\text{H}_a)$ , showing the cross-peak connecting  $\text{H}_a$  and  $\text{P}_a$ ; (d) the  $^1\text{H}$ - $^{31}\text{P}$  spectrum,  $^{31}\text{P}$  decoupled, using  $\tau = \frac{1}{2}J(\text{P}_b\text{H}_b)$ , showing the cross-peak for  $\text{H}_b$  and  $\text{P}_b$ ; (e) the  $^1\text{H}$ - $^{103}\text{Rh}$  correlation spectrum,  $^{103}\text{Rh}$  decoupled, acquired using  $\tau = \frac{1}{2}J(\text{RhH}_a)$  for multiplet selection, showing correlated transitions between  $\text{H}_a$  and  $^{103}\text{Rh}$  in **3**

experiment precludes the observation of the  $\text{H}_a$ - $\text{H}_b$  coupling [ $J(\text{HH}) = -7.5$  Hz] but is sufficient to allow the observation of the rhodium-hydrogen coupling. On acquiring the  $^1\text{H}$ - $^{31}\text{P}$  correlation with the delay  $\tau = \frac{1}{2}J(\text{P}_b\text{H}_b)$ , the observed cross-peak connects  $\text{H}_b$  at  $\delta(^1\text{H}) = -19.5$  to  $\text{P}_b$  at  $\delta(^{31}\text{P}) = -7.4$  [dd,  $J(\text{RhP}_b) = 103$ ,  $J(\text{PP}) = 28$  Hz] [Fig. 1(b) and 1(d)]. In the corresponding  $^1\text{H}$ - $^{103}\text{Rh}$  NMR spectrum of compound **3**, acquired with rhodium decoupling during acquisition [Fig. 1(e)], the hydride at  $\delta(^1\text{H}) = -9.79$  [dt,  $J(\text{P}_a\text{H}_a) = 176$ ,  $J(\text{P}_b\text{H}_a) = -19$  Hz] is connected to the rhodium centre at  $\delta(^{103}\text{Rh}) = -319$  [dt,  $J(\text{RhP}_a) = 88$ ,  $J(\text{RhP}_b) = 103$  Hz].\*

The magnitude of the heteronuclear coupling constants can be measured directly from these spectra; in Fig. 1(a) and 1(b) the peaks are separated by  $J(\text{PH})$  and  $J(\text{RhH})$  in the  $^1\text{H}$  dimension and  $J(\text{PP})$  and  $J(\text{RhP})$  in the  $^{31}\text{P}$  dimension, while in Fig. 1(c) and 1(d)  $J(\text{PH})$  is removed because the spectra are acquired with  $^{31}\text{P}$  decoupling. In the  $^1\text{H}$ - $^{103}\text{Rh}$  spectrum [Fig. 1(e)] the hydride resonances are separated by  $J(\text{P}_a\text{H}_a)$  and  $J(\text{P}_b\text{H}_a)$  in the  $^1\text{H}$  dimension while in the rhodium dimension  $J(\text{RhP}_a)$  and  $J(\text{RhP}_b)$  operate. In addition to this information, the sign of the slope between connected transitions within each cross-peak in the decoupled experiments determines the relative sign of the product of their couplings. It follows that while  $J(\text{RhH}_a)$ ,  $J(\text{RhH}_b)$ ,  $J(\text{RhP}_a)$  and  $J(\text{RhP}_b)$  all have the same sign, the sign of  $J(\text{P}_b\text{H}_a)$  is opposite to this. Spectral analysis therefore reveals

that  $J(\text{P}_b\text{H}_a)$  is negative while the remaining coupling constants are positive [the sign of  $J(\text{PP})$  is unknown].

When a  $z$ -field gradient is used to reduce the phase-cycling requirements of the NMR experiment the new  $^1\text{H}$ - $^{31}\text{P}$  spectrum requires only one scan per increment because these experiments are not signal-limited. Using this simple procedure we are able to quadruple the spectral resolution obtained in the second dimension without increasing the duration of the experiment whilst also reducing the size of spectral artefacts. This result is of critical importance because it allows measurement before relaxation leads to significant depletion of the  $p\text{-H}_2$  spin-state population. Data measurement using all these methods is extremely rapid because the optimum scan-scan repetition time is determined solely by the hydrogen-exchange rate; all these experiments can be completed in less than 3 min of spectrometer time.

The related complex  $[\text{Rh}(\text{PMe}_3)_4]\text{Cl}$  **2** reacts with  $\text{H}_2$  to form  $[\text{RhH}_2(\text{PMe}_3)_4]\text{Cl}$  **4**.<sup>5</sup> When a  $\text{CD}_2\text{Cl}_2$  solution of **2**, under 3 atm of  $p\text{-H}_2$ , is monitored by NMR spectroscopy at 300 K the  $^1\text{H}$  NMR spectrum shown in Fig. 2(a) is obtained immediately. This figure illustrates the *para*-hydrogen-enhanced resonance of the two chemically equivalent, but magnetically inequivalent, hydride ligands of **4**. The anti-phase character seen in these signals is a consequence of the *para*-hydrogen-induced population difference between connected transitions in the  $[\text{AX}]_2$  spin system. In the fully coupled  $^1\text{H}$ - $^{31}\text{P}$  experiment the  $^{31}\text{P}$  resonance for nucleus  $\text{P}_b$  shows passive couplings to rhodium and phosphorus (multiplet selection causes the loss of the central triplet feature) with  $J(\text{RhP}) = 96$  and  $J(\text{PP}) = 28$

\* Both hydrides were observed and show similar doublet of triplet multiplicity in the  $^{103}\text{Rh}$  dimension.

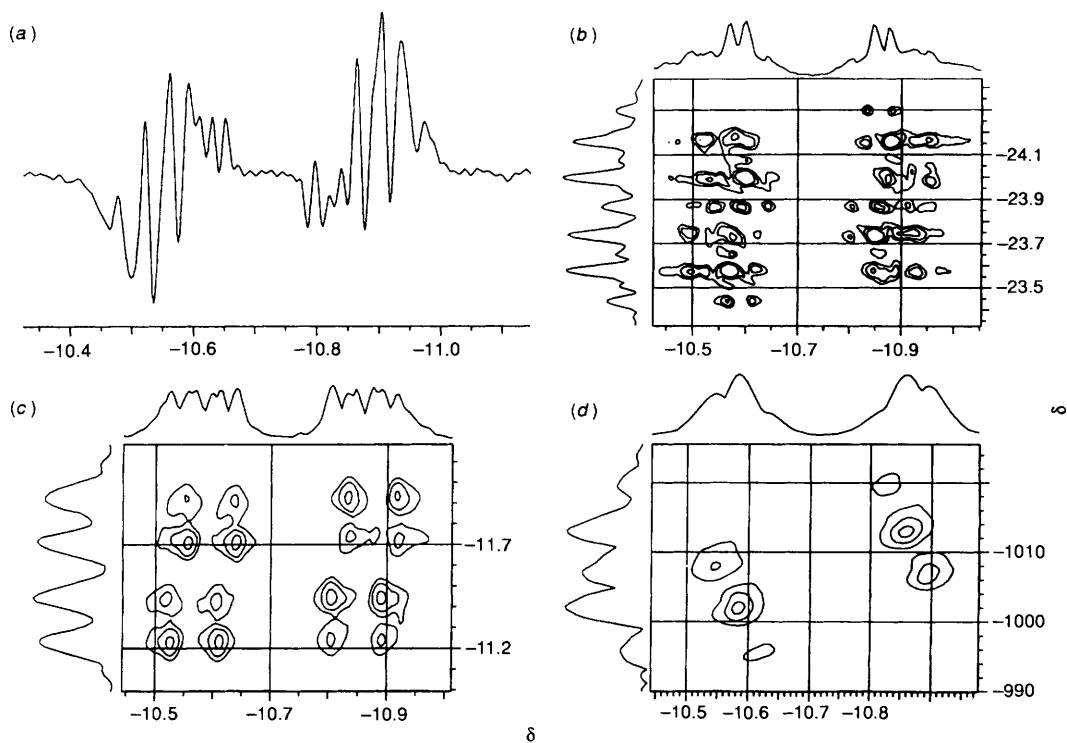


**Fig. 2** The NMR spectra of  $[\text{RhH}_2(\text{PMe}_3)_4]\text{Cl}$  **4** obtained with  $p\text{-H}_2$  in  $\text{CD}_2\text{Cl}_2$  at 300 K: (a)  $^1\text{H}$  (the enhanced anti-phase components arise from transitions within the  $[\text{AX}]_2$  spin system); (b)  $^1\text{H}\text{-}^{31}\text{P}$  correlation acquired using  $J(\text{P}_a\text{H}_a)$  for multiplet selection, showing correlated transitions between  $\text{H}_a$  and  $\text{P}_a$  (positive contours); (c)  $^1\text{H}\text{-}^{31}\text{P}$  correlation acquired with  $\tau = \frac{1}{2}J(\text{P}_b\text{H}_a)$ , showing correlated transitions between  $\text{H}_a$  and  $\text{P}_b$  (absolute value display); (d)  $^1\text{H}\text{-}^{103}\text{Rh}$  correlation,  $^{103}\text{Rh}$  decoupled, using  $J(\text{RhH})$  for multiplet selection, showing correlated transitions between  $\text{H}_a$  and  $^{103}\text{Rh}$  (positive contours)

Hz [Fig. 2(b)]. The higher-field phosphine signal,  $\text{P}_a$  [Fig. 2(c)], appears as a complex multiplet from which  $J(\text{RhP}) = 86$  Hz can be extracted. (These resonances have been simulated using WIN-DAISY.<sup>9</sup>) The corresponding  $^1\text{H}\text{-}^{103}\text{Rh}$  spectrum of compound **4** acquired with rhodium decoupling shows that the hydride at  $\delta(^1\text{H}) - 10.72$  connects to the rhodium centre at  $\delta(^{103}\text{Rh}) - 1007$  [Fig. 2(d)].

When the sample of complex **2** and  $p\text{-H}_2$  was warmed to 325 K additional polarised hydride resonances corresponding to those of **3** were observed, as were signals for the monohydride complex  $[\text{RhH}(\text{PMe}_3)_3\text{Cl}_2]$  **5**, which eventually became the dominant species in solution.<sup>10</sup> Similar results were obtained when samples of **1** and  $p\text{-H}_2$  were warmed to 325 K. In view of the report that **1** and **2** react directly with  $\text{CD}_2\text{Cl}_2$  to yield either  $[\text{Rh}(\text{CD}_2\text{Cl})(\text{PMe}_3)_3\text{Cl}_2]$  or  $[\text{Rh}(\text{CD}_2\text{PMe}_3)(\text{PMe}_3)_2\text{Cl}_3]$  complexes,<sup>11</sup> **3** and **4** must be in equilibrium in  $\text{CD}_2\text{Cl}_2$  under 3 atm  $\text{H}_2$ . We are therefore not able to say whether **3** or **4** is the source of **5** but clearly **1** and **2** must react much faster with  $\text{H}_2$  than with  $\text{CD}_2\text{Cl}_2$ .

These experiments reveal for the first time that  $p\text{-H}_2$  facilitates the acquisition of inverse spectra for highly insensitive nuclei such as  $^{103}\text{Rh}$ . In addition, metal dihydride complexes containing magnetically inequivalent hydride ligands can be detected and identified using this technique. We have also shown that simple field-gradient methods offer dramatic rewards; we are currently using them as spectroscopic filters in the examination of catalytic hydrogenation reactions with  $p\text{-H}_2$ .

#### Acknowledgements

We are grateful to the University of York (for M. G. P.) and the Royal Society for financial support (field-gradient unit and a study visit grant for Australia to S. B. D.). A generous loan

of rhodium trichloride from Johnson Matthey and the loan of a low-frequency probe from Bruker (UK) are gratefully acknowledged. We appreciate helpful discussions with Professor R. Eisenberg.

#### References

- C. R. Bowers and D. P. Weitekamp, *J. Am. Chem. Soc.*, 1987, **109**, 5541.
- R. Eisenberg, *Acc. Chem. Res.*, 1991, **24**, 110.
- S. B. Duckett, C. L. Newell and R. Eisenberg, *J. Am. Chem. Soc.*, 1993, **115**, 1156; 1994, **116**, 10548; S. B. Duckett, R. Eisenberg and A. S. Goldman, *J. Chem. Soc., Chem. Commun.*, 1993, 1185; J. Barkemeyer, M. Haake and J. Bargon, *J. Am. Chem. Soc.*, 1995, **117**, 2927.
- R. A. Jones, F. M. Real, G. Wilkinson, A. M. R. Galas, M. B. Hursthouse and K. M. A. Malik, *J. Chem. Soc., Dalton Trans.*, 1980, 511.
- R. R. Schrock and J. A. Osborn, *J. Am. Chem. Soc.*, 1971, **93**, 2397.
- A. Bax, R. H. Griffey and B. L. Hawkins, *J. Magn. Reson.*, 1983, **16**, 301; M. H. Frey, G. Wagner, M. Vasak, O. W. Sorensen, D. Neuhaus, E. Worgotter, J. H. R. Kagi, R. R. Ernst and K. Wuthrich, *J. Am. Chem. Soc.*, 1985, **107**, 6847.
- O. W. Sorensen, G. W. Eich, M. H. Levitt, G. Bodenhausen and R. R. Ernst, *Prog. Nucl. Magn. Reson. Spectrosc.*, 1983, **16**, 163; G. Wagner, G. Bodenhausen, N. Muller, M. Rance, O. W. Sorensen, R. R. Ernst and K. Wuthrich, *J. Am. Chem. Soc.*, 1985, **107**, 6440.
- G. Drobny, A. Pines, S. Sinton, D. Weitekamp and D. Wemmer, *Faraday Symp. Chem. Soc.*, 1979, **13**, 49; G. Bodenhausen, R. L. Vold and R. R. Vold, *J. Magn. Reson.*, 1980, **37**, 93.
- WIN-DAISY, Brüker-Franzen Analytik, GmbH.
- G. M. Intille, *Inorg. Chem.*, 1972, **11**, 695.
- T. B. Marder, W. C. Fultz, J. C. Calabrese, R. L. Harlow and D. Milstein, *J. Chem. Soc., Chem. Commun.*, 1987, 1543.

Received 1st August 1995; Communication 5/05119C